リサイクル適性Ⓐ
この印刷物は、印刷用の紙へ
リサイクルできます。

# Study on Performance Improvement of a Double-acting Stiring Engine (Performance Evaluation of a New-type Matrix Geometric Pattern)

By Atsushi MATSUGUCHI and Noboru KAGAWA

September 2014

YOKOSUKA, JAPAN

*Memoirs*
*of the National Defense Academy,*
*Japan, Vol. 54, No. 1,*
*(2014), pp. 1-11*

<Paper>

# Study of Performance Improvement of a Double-acting Stirling Engine (Performance Evaluation of a New-type Matrix Geometric Pattern)

By Atsushi MATSUGUCHI* and Noboru KAGAWA**

(Received: March 31, 2014; Accepted for publication: June 13, 2014)

**Abstract**

In this study, the performance and characteristics of several types of a new matrix for a Stirling engine regenerator, called the "mesh sheet," were examined. The mesh sheets were installed in the SERENUM05 3-kW double-acting Stirling engine, and the performance of each matrix was examined from the perspective of engine operation. The specifications of the SERENUM05 engine and its measurement system are described in this paper. Based on the results of our experiments, the characteristic differences between the regenerators of the two-piston and double-acting engines were revealed. As a result, we clarified that the M3 mesh sheet produces the highest indicated efficiency among all the mesh sheets.

**Keywords:** Stirling engine, Double acting, Regenerator, Mesh sheet matrix, Efficiency, Loss

## 1. Introduction

With increased attention being paid to environmental and energy concerns such as climate change, Stirling cycle technology has attracted increased attention. With the aid of heat exchangers that can realize two isothermal processes and a heat-recovery mechanism between the two isochoric processes of the Stirling cycle, the cycle efficiency is higher than that of the thermodynamic cycles of other practical engines. Therefore, the heat exchangers, more commonly known as the “heater” and “cooler,” and the regenerating mechanism, known as the “regenerator,” play an important role. Provided both the heater and cooler can transfer adequate amounts of heat, energy conversion between the engine and high-/low-temperature heat sources can occur efficiently.

Furthermore, the amount of heat supplied to the heater and/or the expansion cylinder can be reduced provided the regenerator can function without any heat loss. To realize a high-efficiency engine, it is essential to design and develop an

*Research Associate; Department of Mechanical Systems Engineering, National Defense Academy
**Professor; Department of Mechanical Systems Engineering, National Defense Academy

optimal heater, cooler, and regenerator for each machine.

A Stirling engine with a high thermal efficiency can be realized by maximizing the efficiency with which energy is stored and recovered. The energy is exchanged with the solid matrix material during the regenerative process. Generally, wire gauze, foam metal, and steel wool (or other random-fiber materials) are used as the regenerator material.

There has been some research into flow analysis and performance using conventional matrix materials. For example, Coppage and London[1)] studied the friction factor and Nusselt number of wire gauze and then went on to summarize the flow friction and heat transfer data. Chen and Griffin[2)] determined a correlation for the normalized friction factor of the wire gauze. Miyabe et al.[3)] and Hamaguchi et al.[4)] presented experimental data on the flow and heat transfer characteristics of stacked wire gauze. Tanaka et al.[5)] showed the flow and thermal performance of wire gauze and other matrix materials in steady and oscillating flows.

Gedeon and Wood[6)] derived correlations between the friction factor and heat transfer coefficient for wire gauze and metal felt in oscillating flows. Zhao and Cheng[7)] measured the pressure drop across wire gauze in oscillating flows. Isshiki et al.[8)] studied the flow resistance and heat transfer of wire gauze in oscillating flows. The major correlations between the flow friction and heat transfer for the conventional matrix material were summarized and compared by Thomas and Pittman[9)].

For a conventional matrix, ready-made material with standardized dimensions is used because of its cost. Therefore, some critical restrictions are imposed on the design of suitable regenerators. However, there have been very few studies that have examined the development of a new matrix material for use in a Stirling engine regenerator.

Our laboratory has developed a “mesh sheet”[10)] material that can be designed with arbitrary dimensions. This mesh sheet is manufactured using advanced etching technology, and a three-dimensional structure can be constructed. Its characteristics were examined using an NS03T 3-kW, 2-piston Stirling engine[11)12)], and the performance was found to be superior to that of conventional wire gauze material[13)].

Based on the available technical information for the NS03T engine, a 3-kW Stirling engine, named SERENUM05, was developed for use in portable generators for both domestic and military applications. The engine is a double-acting type with four pistons, a U-shaped cylinder arrangement, and a unique mechanism. The engine was originally designed at NDA and built in 2005. By adopting this mechanical arrangement and a heat-exchanger system, it initially proved possible to generate 2.2 kW of electrical power with a 24% generating efficiency.

In this study, the performance and characteristics of several types (two geometric patterns) of a new matrix for a Stirling engine regenerator, called a "mesh sheet," were examined. The mesh sheets were installed in the 3-kW double-acting

SERENUM05 Stirling engine and the performance of each matrix was examined from the perspective of engine operation. The results were then compared with the previous results obtained for the two-piston NS03T Stirling engine (a 1984 design) equipped with the mesh sheets[13]. Based on the results of our experiments, the differences between the characteristics of the regenerator of the double-acting and two-piston type engines was clarified. Additionally, the specifications of the SERENUM05 engine are described in this paper.

## 2. Specifications of the SERENUM05 engine

Table 1 lists the design parameters of the developed SERENUM05 engine used in this study. Fig. 1 is a schematic view of the engine. The SERENUM05 engine is a double-acting engine with four pistons. The integrated cylinder block is mounted on a pressurized case. The aluminum case includes a unique mechanism, called a "Z-type crank," and a compact AC generator. The mechanism consists of a Z-shaped crankshaft and a cross-shaped rotator.

The flow passage in each heater and cooler is arranged to realize equally distributed flow patterns and an equivalent flow length. Both the cooler and the regenerator have an annular design and a set of one cooler and one regenerator was inserted into each cylinder as shown in Fig. 1.

Overall, the engine has a diameter of 337 mm and a height of 692 mm. Its mass is about 80 kg including the preheater and AC generator. The engine is described below and the details are listed in Table 2. The specifications and measurement systems for the engine are briefly described below.

**Table 1** Design parameters of 3-kW engine

| | |
|---|---|
| Main fuel | Natural gas |
| Working fluid | Helium |
| Mean pressure | 3 – 5 MPa |
| Max. expansion space temp. | 975 ± 50 K |
| Compression space temps | < 323 K (water cooling) |
| Engine speed | 500 – 1500 rpm |
| Max. output power | > 3 kW |
| Max. generating efficiency | 30 % |
| NOx | <150 ppm |
| Noise level | <60 dB(A) |
| Mass | <80 kg |
| Height | <700 mm |

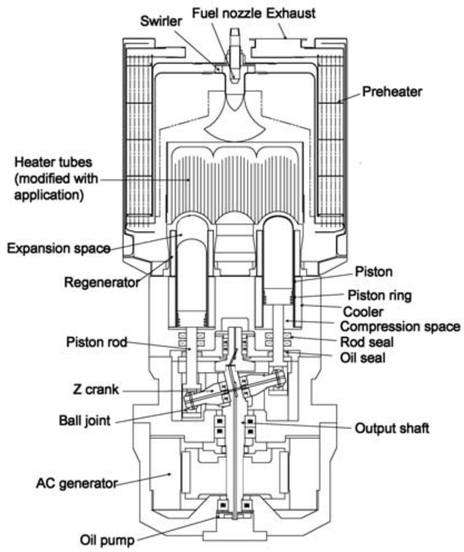


**Fig. 1.** SERENUM05 engine

### 2.1 Combustion systems

The eight-hole fuel injector, swirler, and burner throat realized a short flame length of about 110 mm. The flame exhibits a uniform temperature distribution of the combustion gas, as obtained by a reaction between the natural gas and preheated air. The preheater is a counter-flow type surrounding the combustor to reduce heat loss from the high-temperature side to the ambient air. The combustion gas flows through 180 tubes to heat the fresh air flowing through each annular duct between the concentric cylinder walls.

### 2.2 Heat exchanger system

The heater was constructed from four sets of four heater tubes, which connect the expansion cylinder to the regenerator set in the next cylinder. The heater tubes are of a bayonet type into which an inner core tube is inserted. The tubes are made of Hastelloy X heat-resistant alloy. The temperature difference between each tube is less than 10 K at the average heater wall temperature of 930 K.

The cooler is of a shell and tube type. The cooler has an annular shape located at each cylinder and has eighteen tubes, each of which has an inner core. The tubes and cores were made of copper, the surfaces of which were coated with nickel to prevent corrosion. Cooling water flows around the outside of the cooler tubes. Each tube has longitudinal grooves in its outer surface so that it can shed heat into the water with a higher heat transfer ratio. Helium flows through the 1-mm passage formed by the tube and the core.

The regenerator is an annular type that is 55 mm in length. Stacked stainless-steel 304 mesh sheets are used as the regenerator matrix. In total, there are 500 mesh sheets in the regenerator (Fig. 2). Each screen has three holes, 3 mm in diameter, and three rods are passed through these holes to form the annular regenerator unit. The outer diameter of the regenerator is 65 mm and the inner diameter is 45 mm.

**Table 2** Engine specifications

| | |
|---|---|
| 1. Engine | Double-acting /four cylinders |
| Swept volume | |
| Expansion | 50.9 $cm^3$ x 4 |
| Compression | 44.5 $cm^3$ x 4 |
| Volume Phase angle | 90 degrees |
| Crankcase | Pressurized |
| 2. Combustor | Swirled diffusion burner |
| Combustion capacity | 4.5 – 13 kW |
| Turndown ratio | 1:3 |
| 3. Preheater | Shell and tube |
| Heat transfer area | |
| Combustion gas side | 1.3 $m^2$ |
| Fresh air side | 1.3 $m^2$ |
| 4. Piston Bore | 45 mm |
| Stroke | 32 mm |
| Rod diameter | 20 mm |
| 5. Heater | |
| Heater tube | Bayonet type |
| Material | Hastelloy-X |
| 6. Regenerator | Annular |
| Number | 1 |
| Dead volume | 150 $cm^3$ |
| Heat transfer area | |
| Working fluid side | 0.15 $m^2$ |
| Combustion gas side | 0.23 $m^2$ |
| 7. Matrix | |
| Material | Stainless steel 304/Nickel |
| Mesh | Mesh Sheet |
| Outer & inner diameter | 65 mm, 45 mm |
| Length | 55 mm |
| 8. Cooler | Tube w/core |
| Cooler tube | |
| Outer diameter x Length | 8 mm x 65 mm |
| Number | 18 x 4 |
| Material | Copper |
| Heat transfer area | |
| Working fluid side | 0.07 $m^2$ |
| Water side | 0.28 $m^2$ |
| 9. Piston seal | 3-piece piston ring |
| Ring height | 2.0 mm |
| Stage number | 3 |
| Main material | PTFE |
| 10. Output mechanism | Z-crank |
| Lubrication system | Integrated geared pump |
| 11. Generator | Integrated into crankcase<br>AC, 18 poles |

### 2.3 Drive system

Three-stage, low-friction, and low-wear piston rings are used for the SERENUM05 engine. The three-piece type, which consists of two plane rings, an inner ring, and a steel tension ring, is used for each piston. The plane and inner rings are made of polytetrafluoroethylene (PTFE). Two gas seal (rod) rings and two oil rings are positioned at the bottom of each cylinder where the piston rod reciprocates.

The Z-type crank mechanism consists of a Z-shaped crankshaft and a cross-shaped rotator. The lower part of the piston supports the lateral force loading on the piston rods. Each piston rod has a square rod-end that slides between two linear roller-bearings. At the bottom of the piston, a spherical bearing is used. The bearing has a cylindrical hole through which the arm of the cross-shaped rotator slides. The crankshaft is supported by ball bearing sets. Lubricant is provided by a geared pump with a swept volume of 1 $cm^3$ and is distributed to the major mechanical parts. The compact AC generator with 18 poles, which also acts as a flywheel, is directly attached to the crankshaft.

### 2.4 Measurement systems

Thermocouples, pressure transducers, and crank-angle pickup sensors were installed in the engine. The engine-generated AC power was measured by a wattmeter. A data acquisition system and a digitizer were used to convert the analog signals received from the transducers and sensors to digital signals. Meters measured the fuel (natural gas) flow, combustion air flow, and cooling water flow, and the obtained data was transferred to a personal computer (PC).

The acquisition of the data, calculation of the engine performance, display of the results and the engine operating conditions on the PC screen, and the saving of the data are all automatically performed by software written in a graphical programming language.

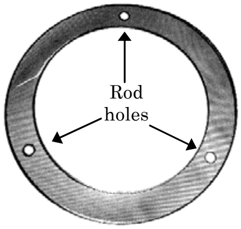


(a) Photograph (M3)

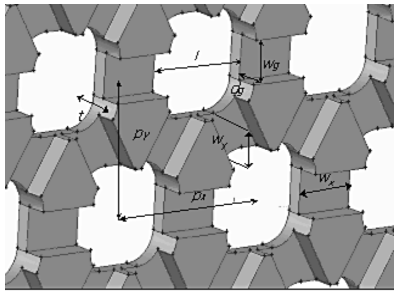


(b) Details

(c) Stacked mesh sheets

**Fig. 2** Mesh sheet

## 3. Mesh sheet specifications and experimental conditions

Seven kinds of mesh sheets were developed for the NS03T two-piston Stirling engine. The mesh sheets are made

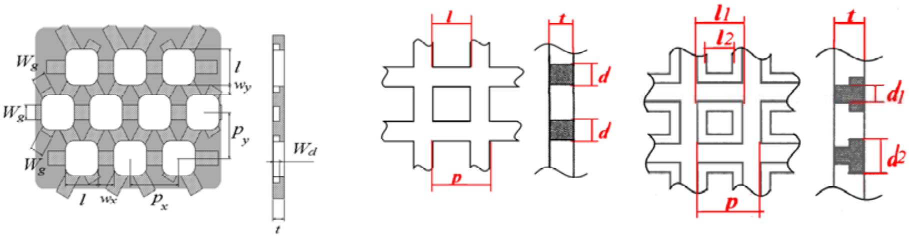


(a)M3 (b) M5 (c) M7

**Fig. 3** Schematic of Mesh Sheet

**Table 3** Geometric constraints of matrix

| Matrix | $l$ | $W_x$ | $W_y$ | $p_x$ | $p_y$ | $t$ | $w_g$ | $w_d$ | $\beta$ | $\phi$ |
|---|---|---|---|---|---|---|---|---|---|---|
| M3 | 0.3 | 0.141 | 0.082 | 0.441 | 0.382 | 0.12 | 0.15 | 0.072 | 0.487 | 0.667 |

| Matrix | $l_1$ | $l_2$ | $d$ | $d_1$ | $d_2$ | $p$ | $t$ | $\beta$ | $\phi$ |
|---|---|---|---|---|---|---|---|---|---|
| M5 | 0.65 | — | 0.15 | — | — | 0.8 | 0.1 | 0.66 | 0.66 |
| M7 | 0.68 | 0.66 | — | 0.1 | 0.12 | 0.78 | 0.1 | 0.738 | 0.738 |

from stainless steel except for the M4 sheet which is made of nickel. Also, the configurations and shapes differ between M1 - M4 (staggered-hole type), M5 (in-line type without grooves), and M6 - M7 (in-line type with grooves). The M3, M5 and M7 types all exhibited good performance when previously installed in the NS03T engine. In this study, they were installed in the SERENUM05 engine, in order to obtain guidelines for the future design of a double-acting engine.

Fig. 3 shows a schematic view of the mesh sheets. The geometric pattern of the M3 type features staggered holes. On the other hand, that of the M5 and M7 types is an in-line design. The number of each type indicates the order in which it was developed. The M3 and M7 types have grooves on one side, in order to reduce the heat conduction and friction losses. All of the mesh sheets used in this study were made of stainless steel (SUS304).

Table 3 lists the dimensional parameters of the mesh sheets, where, $l$, $W_x$, $W_y$, $p_x$, $p_y$, $t$, $w_g$, $w_d$, $l_1$, $l_2$, $d$, $d_1$, and $d_2$ are the dimensions shown in Fig. 3, $\beta$ is the opening ratio, and $\phi$ is the porosity[1)-9)]. The dimensions of the mesh sheets developed after M3 were determined based on numerical analysis results. By using a general-purpose finite element method fluid analysis software, the friction coefficient, $f$, and Nusselt number, $Nu$, were analyzed, while the opening, $l$, width of the frame, $d$, width of the groove, $W_g$, and thickness, $t$, were changed gradually.

**Table4** Operating conditions

| Conditions | |
|---|---|
| Engine speed (rpm) | 600-1000 |
| Heater tube mean temperature (K) | 780 |
| Cooler tube mean temperature (K) | 300 |
| Charged helium pressure (MPa) | 2.0- 2.5 |

**Table 5** Definitions of powers and efficiencies

| Items | Equations |
|---|---|
| 1. Power | |
| Expansion work (power) | $W_e = n\oint P_e dV_e$ |
| Compression work (power) | $W_c = n\oint P_c dV_c$ |
| Indicated work (power) | $W_{ind} = W_e - W_c$ |
| Pressure loss | $\Delta W_p = \left(\oint P_e dV_c + \oint P_c dV_e - W_{ind}\right)/2$ |
| 2. Quantity of heat | |
| Heat input | $Q_{in}$ |
| Cooling heat in cooler (quantity) | $Q_c$ |
| Cooling heat in exp. cylinder. water jacket (quantity) | $Q_{ec}$ |
| Cooling heat in comp. cylinder. water jacket (quantity) | $Q_{cc}$ |
| Regenerator loss | $Q_{rloss} = Q_c + Q_{ec} - W_c$ |
| Effective heat input | $Q_{eff} = Q_{rloss} + W_e$ |
| 3. Efficiency | |
| Indicated efficiency | $\eta_{ind} = W_{ind} / Q_{eff}$ |

Then, the relationship between the porosity, $\phi$, and $f/Nu$ was depicted for each mesh sheet. The size of mesh sheet was determined to minimize the value of $f/Nu$ while keeping $\phi$ was as small as possible[14]. (As $\phi$ increases, the compression ratio and therefore the engine power will decrease).

Table 4 lists the experimental conditions. The engine speed was held at between 600 and 1000 rpm by controlling the electrical load of the AC generator with a newly developed automatic control system. To measure the heater tube mean temperature, three K-type thermocouples were attached to the surface of the heater tubes of each cylinder. They measured the temperatures at the top, middle, and bottom of each tube to maintain the mean temperatures at 780 K. A lower mean temperature was thus obtained for the cooling water inlet and outlet temperatures. The mean temperature was maintained by adjusting the water flow rate. In this study, the pressure of the helium charge was set to between 2.0 and 2.5 MPa.

To confirm the regenerator performance, the engine performance was analyzed by using the measured data. Table 5 lists the definitions of the powers, heats, losses, and efficiencies of the engine. $\Delta W_p$ is the difference between the actual $W_{ind}$ and the calculated $W_{ind}$ when there are no pressure losses. The effective heat input, $Q_{eff}$, and the regenerator loss, $Q_{rloss}$, are derived from the equation in Table 5. As shown in the equation for $Q_{rloss}$, some analyzed heat fluxes in the engine are used for the calculation.

## 4. Experimental results

Figs. 4 to 7 show the experimental results that represent the engine and generator performance. In the figures, $W_{ind}$, $\Delta W_{p}$, and $Q_{rloss}$ are divided by $n \cdot V_{e} \cdot P_{e,mean}$ (where, $n$ is the engine speed, $V_{e}$ is the piston displacement of the expansion volume, and $P_{e,mean}$ is the mean pressure of the expansion volume). Non-dimensional values are shown. This non-dimensionalization is the same technique of dimensional analysis as that proposed by Beal [15].

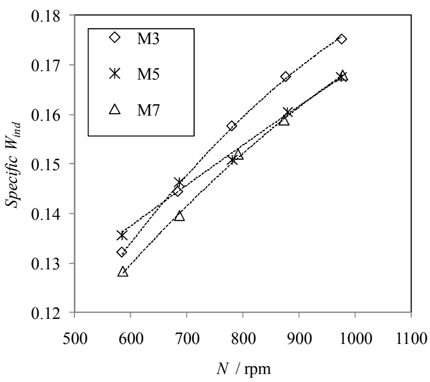


**Fig. 4** Specific indicated work

Fig. 4 shows the relationship between the engine speed and the indicated work, $W_{ind}$ which is the power produced by the actual thermodynamic processes. In this figure, $W_{ind}$ increases with the engine speed. $W_{ind}$ of M3 and M5 mesh sheets similarly increases at engine speeds of between 600 and 700 rpm. However, $W_{ind}$ for M3 becomes larger than the others at higher speeds. Additionally, the value of $W_{ind}$ for M5 and M7 is almost the same between 800 rpm and 1000 rpm.

Fig. 5 shows the pressure loss, $\Delta W_{p}$

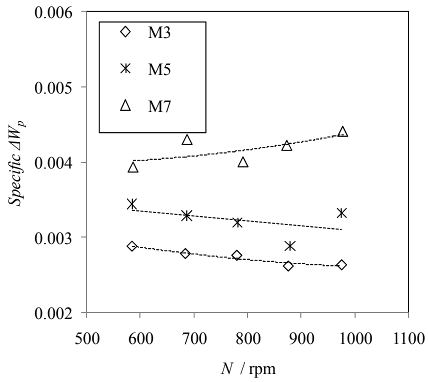


**Fig. 5** Specific pressure loss

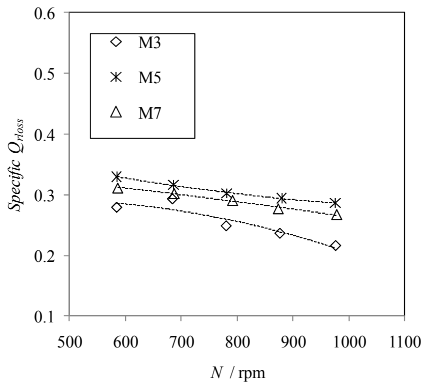


**Fig. 6** Specific regenerator loss

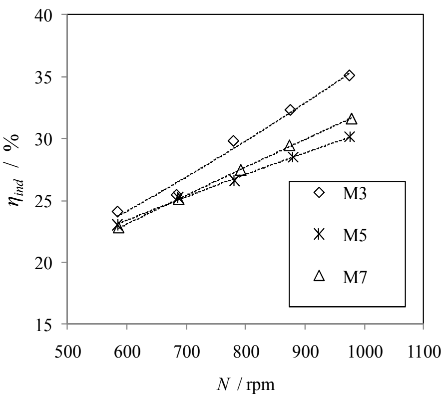


**Fig. 7** Indicated efficiency

required to realize the Stirling cycle. In this figure, although $\Delta W_p$ of M3 is the lowest of all the evaluated mesh sheets, the values of $\Delta W_p$ are very low under every operating condition. These $\Delta W_p$ values are about 10% of those measured with the two-piston NS03T Stirling engine (1984 design)[13].

It is assumed that the way in which the mesh sheets are stacked will lead to a difference in the value of $\Delta W_p$ for the NS03T and SERENUM05 engines. In the case of the SERENUM05 engine, the hole positions of each mesh sheet are aligned with those of the other mesh sheets, because the regenerator is of the annular type, as described in Section 2.2, whereby the mesh sheets are stacked and held in place by three rods in the rod holes that are spaced 120° apart (Fig. 2(a)). Therefore, the helium in the pattern holes flows straight from one end of the regenerator to the other.

On the other hand, the mesh sheets of the NS03T engine are stacked randomly, because the regenerator is of the can type with the sheets fixed by a rod in the center of the mesh sheets[3]. Consequently, the pressure loss in the SERENUM05 regenerator is relatively low.

Fig. 6 shows the results of the experiments regarding regenerator loss caused by the thermal storage process, $Q_{rloss}$. In the figure, $Q_{rloss}$ for M3 is the lowest of all the mesh sheets, and those of M5 and M7 are almost equivalent. From these results, we can assume that the contact surface area between each mesh sheet has a meaningful effect on the heat conduction loss, with the difference in the contact surface area (M5 > M7 > M3) affecting $Q_{rloss}$ of the SERENUM05 engine. Therefore, it would appear that $Q_{rloss}$ is reduced by the grooves in the mesh sheet.

Additionally, it is clear that $Q_{rloss}$ for the SERENUM05 engine is about four times that of the NS03T engine[13] even though the heat conduction loss is reduced by the grooves in each mesh sheet. The reason for this seems to be the direct flow of the helium through the SERENUM05 regenerator.

Fig. 7 shows the results of the experiments related to the indicated efficiency, $\eta_{ind}$, which is the thermodynamic efficiency of the actual Stirling cycle. In this figure, $\eta_{ind}$ of M3 has the highest value among the evaluated matrixes. The performance difference increases at higher engine speeds. From Figs. 5, 6, and 7, it is noted that $\eta_{ind}$ is improved by reducing $\Delta W_p$ and $Q_{rloss}$.

## 5. Conclusions

In this study, the performance and characteristics of the three types of the new matrixes for the mesh sheets of the Stirling engine regenerator were examined by being applied to the SERENUM05 3-kW double-acting Stirling engine. Based on the results of our experiments, the characteristic difference between the regenerators of the two-piston and double-acting type engines became clear. As a result, we can draw the following conclusions.

(1) The regenerator using the M3 mesh sheets with the staggered pattern and the grooves has the highest indicated

efficiency for the SERENUM05 engine.

(2) The regenerator loss, $Q_{rloss}$, is reduced by the grooves in the mesh sheet.

The new knowledge obtained by this study will be useful for developing a high-performance matrix for Stirling engine regenerators.

## Acknowledgment

The authors thank Kenji Kitayama of Akebono Kikai Co., Ltd. for his technical advice in developing the mesh sheets. The authors also acknowledge Johnan Corp. and Kenichi Tamura of the Japan Defense Foundation for Mutual Aid for their technical support.

## References

1) Coppage JE, London AL. “Heat transfer and flow friction characteristics of porous media”, *Chemical Engineering Progress.* **52**[2](1956), pp.57-63.

2) Chen NCJ, Griffin FP. “Effect of pressure drop correlations on Stirling engine predicted performance”, *Proceedings of 18th IECEC.* (1983), pp.708-713

3) Miyabe H, Takahashi S, Hamaguchi K. “An approach to the design of Stirling engine regenerator matrix using packs of wire gauze”, *Proc. 17th IECEC.* (1982), pp.1839-1844.

4) Hamaguchi K, Takahasi S, Miyabe H. “Flow losses of regenerator matrix - Case of packed wire gauges”, *Trans. Japan Society of Mechanical Engineers.* **B48**[435](1982), pp. 2207-2216 (in Japanese).

5) Tanaka M, Yamashita I, Chrisaka F. “Flow and heat transfer characteristics of the Stirling engine regenerator in an oscillating flow”, *JSME Int. J.* Series II **33**[2](1990), pp.283-289.

6) Gedeon D, Wood JG. “Oscillating-flow regenerator test rig - Hardware and theory with derived correlations for screens and felts”, *NASA Contractor Report.* **198442** (1996).

7) Zhao TS, Cheng P. “Oscillatory pressure drops through a woven-screen packed column subjected to a cyclic flow”, *Cryogenics.* **36**[5](1996), pp.333-341.

8) Isshiki S, Ushiyama I, Sakano A, Isshiki N. “Studies on flow resistance and heat transfer of regenerator wire meshes of Stirling engine in oscillatory flow”, *JSME Int. J.* **B40**[2](1997), pp.281-289.

9) Thomas B, Pittman D. “Update on the evaluation of different correlations for the flow friction factor and heat transfer of Stirling engine regenerators”, *Proc. 35th IECEC.* **1** [AIAA-2000-2812] (2000), pp.76-84.

10) Kagawa N, Takizawa H. Japanese Patent No. 3677551(2004).

11) Kagawa N, Sakamoto M, Nagatomo S, Komakine T, Hisaoka S, Sakuma T, Arai Y, Okuda M. “Development of a 3 kW Stirling engine for a residential heat pump system”, *Proc. 4th ISEC.* (1988), pp.1-6.

12) Kagawa N. “Experimental study of 3-kW stirlng engine”, *Journal of Propulsion and Power.* **8**[3](2002), pp.696-702.

13) Takizawa H, Kitahama D, Kagawa N, Matsuguchi A, Tsuruno S. “Development of new matrix material for Stirling engine regenerator”, *Trans. Japan Society of Mechanical Engineers.* **B70**[691](2004), pp.823-828 (in

Japanese).
14) Matsuguchi A., Izumi T., Kitahama D., Takeuchi T., Kagawa N. "Design and Development of New Matrix for Stirling Engine Regenerator", *Proc. 2nd IECEC* CD-ROM. AIAA-2004-5601(2004).
15) Walker G. "Stirling Engines", Clarendon Press, London, (1980).